Journal of Zhejiang University-SCIENCE B 2026 27(7):715-735
www.jzus.zju.edu.cn; www.springer.com/journal/11585
E-mail: jzus_b@zju.edu.cn

Review

https://doi.org/10.1631/jzus.B2500786

Check for updates

Blood–brain barrier permeability assessment: from biomimetic models to multimodal imaging

Miaomiao WANG[1], Lu GAN[1], Yiru FAN[1], Chenxi DUAN[2,3], Ying ZHU[1], Shihua LUO[4]✉, Yanhong SUN[1]✉

[1]*Institute of Materiobiology, College of Sciences, Shanghai University, Shanghai 200444, China*
[2]*Shanghai Institute of Applied Physics, Chinese Academy of Sciences, Shanghai 201800, China*
[3]*University of Chinese Academy of Sciences, Beijing 100049, China*
[4]*Department of Traumatology, Rui Jin Hospital, School of Medicine, Shanghai Jiao Tong University, Shanghai 200025, China*

Abstract: The blood–brain barrier (BBB) is a vital physiological structure that maintains the microenvironmental homeostasis in the central nervous system (CNS). Imbalances in its permeability play a key role in various neurological disorders, including stroke, neurodegenerative diseases, and brain tumors. The development of precise techniques for assessing BBB permeability is therefore paramount for elucidating the mechanisms of neurological diseases, overcoming drug development challenges, and achieving precise diagnosis and treatment of CNS disorders. This review systematically summarizes the latest advances in the assessment of BBB permeability. Regarding in vitro models, platforms have evolved from the traditional transwell system to microfluidic chips incorporating fluid shear forces and subsequently to highly biomimetic brain organoids, with continuous improvements in the ability to simulate the neurovascular unit (NVU) microenvironment. For in vivo assessment, we detail the principles and applications of imaging techniques, including dynamic contrast-enhanced magnetic resonance imaging (DCE-MRI), positron emission tomography (PET), near-infrared II (NIR-II) fluorescence imaging (FI), and two-photon microscopy (TPM), highlighting their complementary strengths in macroscopic quantification, molecular targeting, and microscopic dynamic observation. The integration of multi-modal technologies and precise quantitative assessment is a prominent trend. Future investigations will focus on artificial intelligence (AI)-driven personalized permeability assessment, the development of novel intelligent probes, and the dynamic real-time monitoring of the BBB, thereby providing powerful methodological support for neurological disease research.

Key words: Blood–brain barrier (BBB); Permeability assessment; In vitro BBB model; In vivo imaging; Central nervous system (CNS)

1 Introduction

The blood–brain barrier (BBB) is a highly selective, semipermeable structure that separates the blood circulatory system and the central nervous system (CNS). By regulating the exchange of substances, it helps maintain the homeostasis of the cerebral microenvironment (He et al., 2018; Wu et al., 2023; Liu et al., 2025). The BBB primarily comprises endothelial cells, astrocytes, pericytes, and the basement membrane (Fig. 1). Brain microvascular endothelial cells (BMECs) constitute the core component of the BBB. They form a continuous physical barrier through intercellular connections, mainly tight junctions and adherens junctions. Tight junctions consist of transmembrane proteins that are linked to the actin cytoskeleton via cytoplasmic scaffolding proteins. They are responsible for maintaining selective permeability and controlling tissue homeostasis (Anderson and van Itallie, 2009; Luissint et al., 2012; Dong, 2018; Ahlawat et al., 2020). Adherens junctions, mainly constituted by vascular endothelial (VE)-cadherin and its intracellular binding partners such as β-catenin, are instrumental in regulating intercellular adhesion strength and barrier integrity (Vorbrodt and Dobrogowska, 2003; Turowski and Kenny, 2015; Stamatovic et al., 2016; Malinova

✉ Shihua LUO, jqab@163.com
Yanhong SUN, sunyanhong@shu.edu.cn
Shihua LUO, https://orcid.org/0009-0008-0862-5132
Yanhong SUN, https://orcid.org/0000-0002-1774-8598
Miaomiao WANG, https://orcid.org/0009-0007-3819-9958

Received Dec. 1, 2025; Revision accepted Mar. 12, 2026; Crosschecked June 16, 2026

and Huveneers, 2018). Studies have shown that when these junctional proteins are downregulated or dysfunctional, BBB permeability becomes abnormal, which can contribute to various neurological disorders (Krol et al., 2013). Astrocytes envelop the cerebral microvasculature with their endfeet. By secreting diverse signaling molecules, they induce tight junction formation among endothelial cells and maintain barrier properties (Zhao et al., 2015; Schurhoff and Toborek, 2023). Pericytes are embedded in the capillary basement membrane and envelop the endothelial cells. They can modulate capillary blood flow by contracting, and they also participate in the development, homeostatic maintenance, and repair of barrier function (Bell et al., 2010; Kisler et al., 2017; Kadry et al., 2020). The basement membrane, a dense extracellular matrix network, provides structural support for the BBB's cellular components and mediates cell–matrix interactions to regulate its permeability (Bayir et al., 2019).

As a physiological interface, the BBB allows the passage of water and certain small molecules while effectively excluding the majority of large-molecular-weight substances. This selective impermeability protects the CNS from toxins, pathogens, and metabolic waste present in the systemic circulation, while also restricting the nonspecific permeation of neurotransmitters and hormones. As a result, it provides a highly stable internal environment for neuronal activity (Bhattacharya et al., 2020; Segarra et al., 2021). For instance, specific ion channels and transport proteins at the BBB meticulously regulate ion flux between the blood and brain tissue (Harilal et al., 2020; Yang et al., 2020). This precise regulation maintains ionic balance and pH homeostasis between the blood and cerebrospinal fluid, ensuring an optimal cerebral microenvironment. The BBB also actively delivers essential nutrients to the brain via specialized transport proteins, meeting its high metabolic demands. For example, the glucose transporter type 1 (GLUT1) efficiently moves glucose—the brain's primary energy source—from the blood into the CNS. Similarly, the L-type amino acid transporter 1 (LAT1) mediates the uptake of large neutral amino acids (de Vivo et al.,

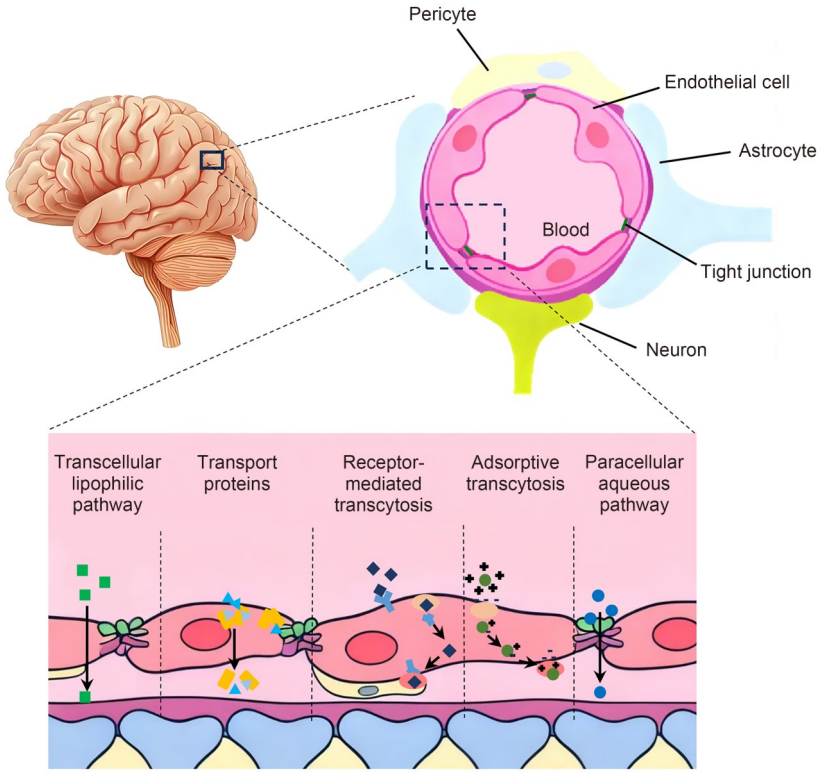

Fig. 1 Schematic of the blood–brain barrier (BBB) structure and key transport pathways. The BBB comprises endothelial cells interconnected with tight junctions, and is supported by pericytes and astrocytic endfeet. The schematic highlights the principal pathways of substance traversal: the transcellular route (including lipophilic diffusion and transcytosis) and the restricted paracellular aqueous pathway.

1991). In terms of active defense, the BBB expresses various efflux transporters, such as P-glycoprotein (P-gp) and breast cancer resistance protein (BCRP). These pump xenobiotics and metabolic byproducts back into the bloodstream, preventing harmful substances from accumulating in the brain (Balzer et al., 2022). Recent studies have further elucidated the BBB's role in the glymphatic system, a paravascular pathway responsible for cerebrospinal and interstitial fluid circulation. This process relies on aquaporin-4 (AQP4) water channels located on astrocytic endfeet, which promote the convective flow of cerebrospinal fluid (CSF) through the brain parenchyma and facilitate interstitial solute clearance. This mechanism is recognized as essential for maintaining a clean internal cerebral environment (Iliff et al., 2012).

The selective permeability of the BBB is not only essential for CNS homeostasis but also plays a key role in the pathogenesis and treatment of various CNS disorders. Many studies have demonstrated that BBB dysfunction is a central pathological event in several neurological diseases. For instance, amyloid-β (Aβ) is a primary pathological protein in Alzheimer's disease (AD). The production and deposition of Aβ strongly influence the progression and prognosis of AD, and this process is closely related to the BBB's diminished capacity to clear Aβ. Furthermore, Aβ deposition can damage the structure of the BBB, establishing a vicious cycle of "Aβ deposition–BBB impairment–attenuated clearance ability–further Aβ accumulation," thereby accelerating disease progression (Wang et al., 2021). Consequently, in addition to their role in the pathogenesis of CNS diseases, changes in BBB permeability can serve as diagnostic indicators and prognostic biomarkers for associated disorders. BBB permeability is also a factor in drug development, as it affects the therapeutic efficacy of interventions for CNS diseases. Although an intact BBB effectively prevents most blood-borne substances from entering the brain, it also blocks most therapeutic agents. It is estimated that over 98% of small-molecule drugs and nearly all large-molecule biologics fail to cross the BBB and reach brain tissue at clinically relevant concentrations, presenting a major bottleneck in the treatment of diseases such as stroke, neurodegenerative diseases, brain tumors, meningitis, and multiple sclerosis (Banks, 2016; Pandit et al., 2020). Hence, advanced techniques for assessing BBB permeability are essential for the early screening of candidate compounds with favorable brain penetration potential, thereby enhancing the success rate and efficiency of CNS-targeted drug development programs.

Developing reliable methods to assess BBB permeability is essential for understanding CNS pathologies and discovering new therapies (Ahlawat et al., 2020; Zheng et al., 2024). Major breakthroughs in detection technologies have been made in recent years, ranging from in vitro models to in vivo imaging. This review summarizes recent progress, compares the advantages and limitations of various technologies, and offers methodological guidance and conceptual frameworks for research on BBB structure, CNS disorders, and therapeutic strategies.

2 In vitro assessments of BBB permeability

2.1 In vitro BBB model

The construction of in vitro BBB models that accurately simulate the physiological parameters and molecular characteristics of the neurovascular unit (NVU) provides a key tool for studying the pathological mechanisms and screening potential drugs for CNS diseases. Driven by microfluidics and organoid technologies, the field of in vitro BBB models has seen major advances in recent years. This has led to a transition from traditional monolayer, two-dimensional (2D) co-culture systems toward three-dimensional (3D) biomimetic systems that more closely simulate the in vivo microenvironment (Sivandzade and Cucullo, 2018). Presently, two main types of in vitro models are used to assess BBB permeability: static models based on transwell chambers and dynamic models (Table 1).

2.1.1 Static BBB model

The static model is the most widely used in vitro BBB model. It is constructed by incubating BMECs on the porous membrane of a transwell insert. To assess barrier permeability, the apparent permeability coefficient (P_{app}) is calculated by measuring the translocation of test substances from the apical (luminal) compartment to the basolateral compartment. Based on the cellular composition, static BBB models are further classified into two principal categories: monoculture and co-culture systems (Fig. 2) (Bagchi et al., 2019). The simplest monoculture model initially used primary

Table 1 Comparison of in vitro BBB models

In vitro model	Cell composition	Physiological functions and characteristics	Physiological fidelity	Primary application scenarios
Static model				
Monoculture	Endothelial cells	Reflects basic barrier properties; low TEER	Low	Study of signaling pathways, transporter kinetics, binding affinity, and high-throughput screenings
Co-culture	Endothelial cells, astrocytes, and pericytes	Enables partial biochemical signal responses through fluid exchange; improved TEER	Medium	Standard permeability assays and mechanistic studies
Dynamic model				
Cone-plate BBB apparatus	Endothelial cells (expandable to co-culture)	Applies controlled shear stress; TEER can be modulated	Medium	Hemodynamic study
Hollow fiber bioreactors	Endothelial cells and astrocytes/pericytes (3D co-culture)	Dynamic perfusion provides shear stress, supports sustained high barrier function, and allows for long-term responsiveness to circulating factors/drugs	High	Validation and optimization of lead compounds in drug discovery
Microfluidics (BBB-on-a-Chip)	Endothelial cells, astrocytes, pericytes, and other NVU cells (controllable 3D co-culture)	Highly controllable system capable of integrating shear force, chemical gradients, and real-time monitoring	High	High spatiotemporal resolution research on mechanisms, drug evaluation, and disease modeling
Brain organoids	Endothelial cells, pericytes, astrocytes, neurons, and microglia (self-organized or engineered a complete NVU)	Designed to replicate complex cell–cell interactions and pathophysiological responses	High	Research on complex brain diseases and exploration of individualized treatment

BBB: blood–brain barrier; TEER: transendothelial electrical resistance; 3D: three-dimensional; NVU: neurovascular unit.

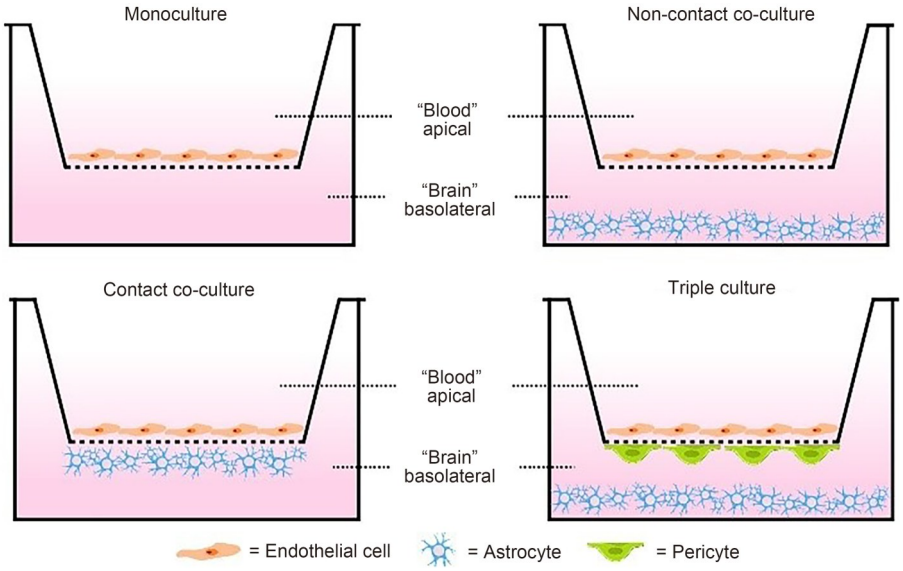

Fig. 2 Schematic of four common static in vitro models of the blood–brain barrier (BBB). These transwell-based models vary in cellular complexity. Monoculture consists of only brain microvascular endothelial cells (BMECs). Co-culture models consist of BMECs and astrocytes. In the non-contact co-culture model, BMECs are seeded on the transwell membrane while astrocytes are cultured in the basolateral compartment, allowing paracrine signaling. In the contact co-culture model, BMECs are grown in direct physical contact with an astrocyte layer. In the triple culture model, BMECs are co-cultured with both astrocytes and pericytes, thereby best recapitulating the native neurovascular unit. The apical chamber represents the "blood" side, and the basolateral chamber represents the "brain" side.

BMECs isolated from rats, cows, or pigs. A key advantage is that these primary cells retain essential BBB characteristics, such as well-defined tight junctions and the polarized expression of various transporters (Cecchelli et al., 2007). To circumvent the limitations of primary cells—namely, low yield and susceptibility to contamination—immortalized cell lines (e.g., human cortical microvessel endothelial cell/D3 [hCMEC/D3]) have been widely adopted (Muruganandam et al., 1997; Weksler et al., 2013). However, these cell lines often exhibit an incomplete barrier phenotype, frequently necessitating functional enhancement with compounds such as cyclic adenosine monophosphate (cAMP) or glucocorticoids to improve barrier properties (Hurst and Fritz, 1996; Franke et al., 1999; Naik and Cucullo, 2012; Daniels et al., 2013). The monoculture model is simple to operate and well suited for high-throughput drug screening and basic mechanistic studies. Its main limitations are the lack of synergistic interactions with other NVU cells and the inability to simulate hemodynamic shear stress. Consequently, it can not fully mimic the complex functions of the in vivo BBB (Mantecón-Oria et al., 2022b). Co-culture models address the shortcomings of monoculture systems. Co-culturing BMECs with astrocytes promotes tight junction maturation and reduces pinocytosis activity (Rubin et al., 1991; Dohgu et al., 2005). Further introduction of pericytes to form a triple-culture model enables the secretion of factors such as transforming growth factor-β (TGF-β), which synergistically increase transendothelial electrical resistance (TEER), lower passive permeability, and enhance efflux transporter activity. It is currently regarded as the static model that most closely mimics the in vivo BBB (Nakagawa et al., 2009).

2.1.2 Dynamic BBB model

The dynamic model can better mimic the mechanical microenvironment of the BBB in vivo by introducing fluid shear stress (Fig. 3). Studies have shown that applying shear stress upregulates the expression of tight junction proteins, such as zonula occludens protein 1 (ZO-1), and thus enhances barrier integrity (Bagchi et al., 2019). Representative dynamic BBB platforms include the cone-plate BBB apparatus (Naik and Cucullo, 2012), hollow fiber bioreactors (Stanness et al., 1997; Janigro et al., 1999; Cucullo et al., 2008; Nogueira et al., 2021), microfluidics (Jiang et al., 2019; Oddo et al., 2019; Wang et al., 2020; Hajal et al., 2022), and organoids (Bergmann et al., 2018; Logan et al., 2019; Dao et al., 2024). The cone-plate BBB apparatus uses a rotating cone to impose a defined shear stress on endothelial cells, facilitating the study of their mechanoresponse. However, its utility in modeling the BBB is limited by its inherent inability to incorporate the multicellular crosstalk essential for a fully functional NVU. In contrast, hollow fiber bioreactors use a 3D tubular design. BMECs are seeded on the luminal surface of semipermeable hollow fibers. Culture medium is perfused through the fiber lumen to generate physiological shear stress, while astrocytes or pericytes can be co-cultured within the extracapillary space (Cucullo et al., 2011). This 3D tubular architecture extends the viable culture period of the model (from days to months) and induces cells to form in vivo-like morphologies and more complex connections (Neuhaus et al., 2006).

In recent years, dynamic models have become more complex and physiologically relevant to better reflect human physiology and improve predictive value (Banerjee et al., 2016; Mantecón-Oria et al., 2020). For instance, polycaprolactone/graphene (PCL/G) composite materials have been explored to promote astrocyte differentiation (Mantecón-Oria et al., 2022a), and transparent polyvinylidene fluoride (PVDF) hollow fibers now enable real-time, non-invasive cell observation (Mantecón-Oria et al., 2025). However, hollow fiber models still face challenges in mimicking in vivo tissue complexity and fluid dynamics, making it difficult to accurately reproduce physiological shear forces and pulsatile flow fields. In contrast, microfluidic technology offers high integration, controlled fluid environment, and 3D architectures, making it a research focus (Mármol et al., 2023; Ceccarelli et al., 2024; Sun and Song, 2024; Sonninen et al., 2025). A common design incorporates parallel channels for the co-culture of endothelial cells, pericytes, and astrocytes to investigate the trans-barrier transport mechanisms of nanoparticles or antibodies (e.g., transferrin receptor targeting) (Wevers et al., 2018). More advanced systems enable the fabrication of 3D tubular vascular structures and have been employed to quantitatively assess the permeability of peptides such as apolipoprotein E (ApoE) and to determine drug permeability by liquid chromatography-tandem mass spectrometry (LC-MS/MS), with data consistent with in vivo studies.

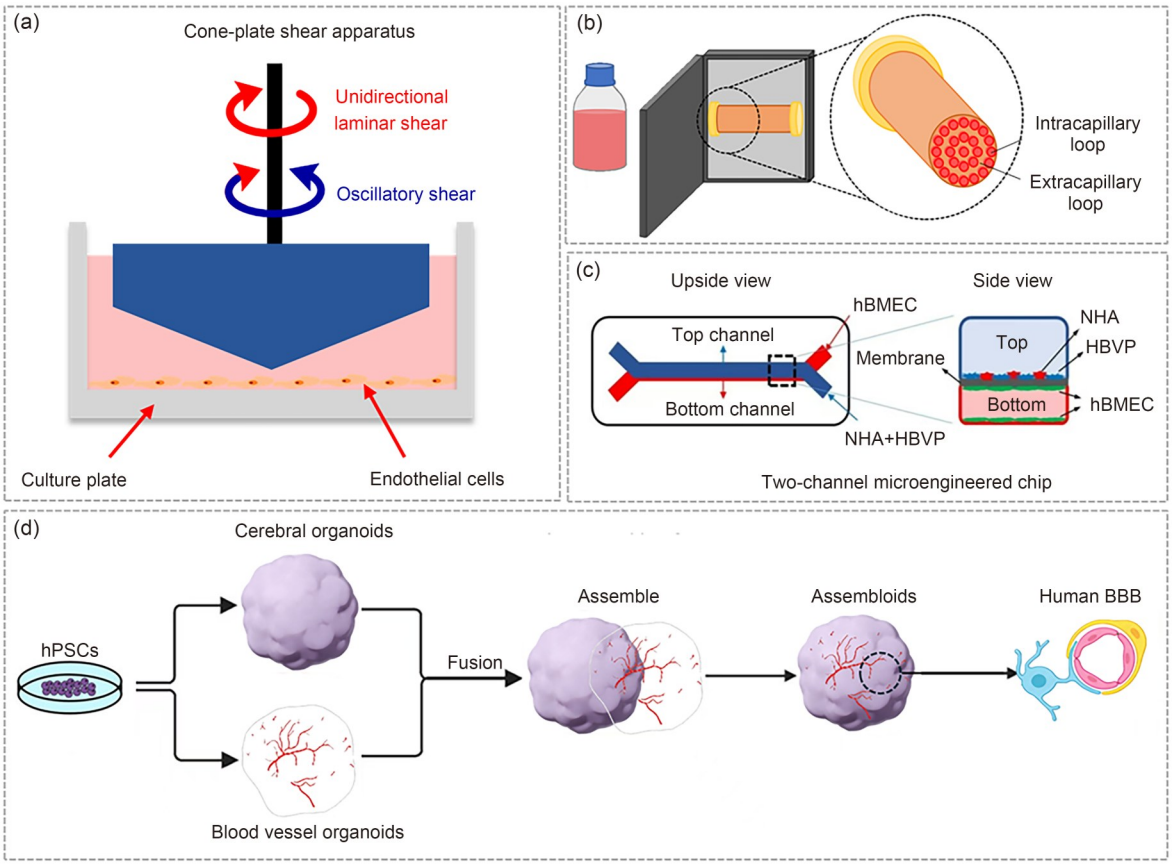

Fig. 3 Dynamic blood–brain barrier (BBB) model. (a) Cone-plate BBB apparatus. (b) Schematics of a hollow fiber bioreactor system and a close-up of the hollow fiber module, comprising an outer sheath and internal fibers. Cells can adhere to the fiber surface, enabling mass transfer through the semipermeable membrane. Reprinted from Nogueira et al. (2021), Copyright (2021), with permission from MDPI. (c) A two-channel microengineered chip had human brain microvascular endothelial cells (hBMECs, green) on all surfaces of the bottom channel, and normal human astrocytes (NHAs, red) and human brain vascular pericytes (HBVPs, blue) on the surface of the top channel. Reprinted from Yang et al. (2024), Copyright (2024), with permission from MDPI. (d) Schematic protocol for generating three-dimensional (3D) human BBB assembloids from cerebral organoids and blood vessel organoids. hPSCs: human pluripotent stem cells.

This demonstrates their potential for substituting animal experiments during early-stage drug development (Chung et al., 2020; Yang et al., 2024). However, microfluidic models have yet to fully replicate the multicellular interactions, dynamic blood flow, and long-term stability of the native BBB due to limited structural complexity and physiological realism.

Organoids are another rapidly developing type of BBB model. They are widely applied in drug delivery and disease modeling due to their highly biomimetic characteristics. For instance, Nzou et al. (2018) developed a 3D human cortical spheroid BBB model with six major brain cell types (endothelial cells, pericytes, astrocytes, etc.), showing tight junctions and charge selectivity. This model is useful for neurotoxicity screening and hypoxic disease modeling, providing a more human-relevant in vitro platform for drug development. To improve throughput and reproducibility, Simonneau et al. (2021) engineered a high-throughput BBB organoid platform based on a hydrogel microwell array. Co-culturing the three core cell types generates thousands of uniform organoids in a single experiment, with semi-automated imaging. Notably, this study first applied clustered regularly interspaced short palindromic repeats (CRISPR)/CRISPR-associated protein 9 (Cas9) system on this platform to reveal the molecular mechanisms governing the BBB penetration of specific antibodies. This approach provides an efficient tool for the large-scale screening of CNS-targeting antibodies and for analyzing their transport mechanisms.

Although 3D models better reflect the human BBB, challenges remain: lack of standardized protocols,

limited maturity, and poor long-term stability of the barriers. Overcoming these obstacles will likely require a synergistic strategy that combines the controllability of microfluidics with the biological authenticity of organoids, paving the way for advances in CNS drug development and disease modeling.

2.2 Techniques for evaluating the permeability of in vitro BBB models

In studies of in vitro BBB models, accurate assessment of the barrier permeability is essential. Currently, the two most common and accepted methods for functional validation are P_{app} and the measurement of TEER (Fig. 4).

2.2.1 P_{app} determination of in vitro BBB models

The principle of P_{app} determination involves quantitatively measuring the transport rate of a specific substance across a cellular monolayer under controlled conditions to assess barrier function. Its advantages include operational simplicity, low cost, and ease of implementation for high-throughput screening. It also allows simultaneous use of tracer molecules with different molecular weights to evaluate the BBB's size-dependent selectivity. For instance, Ito et al. (2019) co-cultured human BMECs with astrocytes and pericytes in a transwell system to build a functional in vitro BBB model. Using unidirectional transport assays, they found that P_{app} values for highly permeable drugs were substantially higher than those for low-permeability markers, spanning a 287-fold range. Compared to monoculture, the triple-culture model exhibited a tighter barrier and better function of efflux transporters such as P-gp. This model provides a reliable tool for assessing the brain penetration in CNS drug discovery. Appelt-Menzel et al. (2017) determined P_{app} values to characterize the barrier properties of a stem cell-derived BBB model. Hydrophilic markers of different molecular weights revealed a molecular-weight-dependent permeation profile: P_{app} values decreased from approximately 1.5 μm/min for small molecules to 0.0030 μm/min for 40 kDa dextran. Transcellular permeability and active transport function of reference drugs were evaluated with P_{app} values normalized to that of diazepam. The quadruple-culture model had the tightest barrier and lower permeability for large molecules than monocultures. Adding verapamil (a P-gp inhibitor) increased the P_{app} value of its substrate rhodamine 123, confirming functional, correctly polarized efflux transporters. These systematic P_{app} determinations demonstrate that the quadruple-co-culture BBB model exhibits excellent barrier integrity and holds potential for predicting drug permeability.

2.2.2 TEER measurement of in vitro BBB models

TEER measurement is a key method for assessing the integrity and permeability of cellular monolayers (Deli et al., 2005; Benson et al., 2013). It quantifies electrical resistance across a cell layer, offering high sensitivity and real-time monitoring. It can detect early-stage, subtle alterations in barrier function induced by pharmaceuticals, cytokines, or pathological conditions. Furthermore, TEER enables longitudinal, dynamic tracking of barrier function in the same samples during drug screening or disease modeling. It directly reflects the barrier's physiological functional state rather than merely reporting protein expression levels. TEER measurement techniques are broadly categorized into two approaches: the Ohm's Law

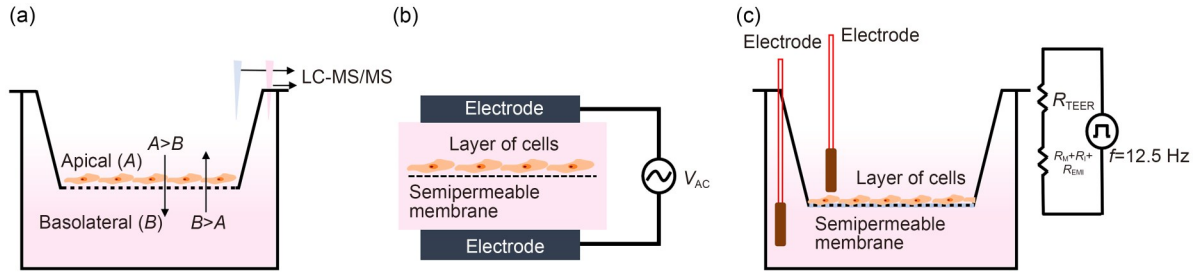

Fig. 4 Permeability assessment of the in vitro blood–brain barrier (BBB) model. (a) Measurement of the apparent permeability coefficient (P_{app}). (b) Measurement of transendothelial electrical resistance (TEER) using impedance spectroscopy. (c) Measurement of TEER using Ohm's Law. The total electrical resistance includes ohmic resistance of the cell layer (R_{TEER}), cell culture medium (R_M), semipermeable membrane insert (R_I), and electrode medium interface (R_{EMI}). V_{AC}: alternating current voltage; f: frequency; LC-MS/MS: liquid chromatography-tandem mass spectrometry.

method and impedance spectroscopy (Srinivasan et al., 2015; Nazari et al., 2023). The Ohm's Law method applies an alternating current across electrodes on either side of the cell layer, measures the resistance, and multiplies it by the membrane surface area to obtain the TEER value, which is then normalized to that of a blank control. A higher resistance corresponds to a greater TEER value, indicating a more intact barrier. The Ohm's Law method is simple, but its measurements are affected by electrode position and current density uniformity. Conversely, impedance spectroscopy applies a small-amplitude alternating current excitation signal with frequency sweeps and measures the resulting current's amplitude and phase response. By scanning frequencies and fitting the data to equivalent circuit models, it captures more comprehensive electrical properties and provides a more accurate TEER value (Douville et al., 2010).

TEER measurement technology is advancing toward standardization, integration, and high-throughput capabilities. For example, van der Helm et al. (2016) developed a four-electrode TEER system for direct quantification in organ-on-a-chip platforms. Six distinct electrode configurations are employed for measurements, and a derived formula is used to directly calculate the resistance of the cellular barrier and the membrane, effectively eliminating background noise from microchannel resistance. In an hCMEC/D3 cell-based BBB-on-a-chip model, stable, reliable TEER measurements (22 $\Omega \cdot cm^2$) were achieved, consistent with traditional transwell results (Malik et al., 2025). This approach does not interfere with microscopic observation, enhancing the reliability of quantitative barrier function assessment on organ-on-a-chip platforms. Separately, Badiola-Mateos et al. (2021) introduced a multi-frequency TEER sensor array for real-time monitoring of BBB integrity. This technology integrates a microfluidic chip with embedded gold electrodes and couples it with broadband impedance spectroscopy, acquiring impedance data across a frequency range of 100 Hz to 10 MHz. By incorporating a machine learning algorithm, the system enables high-precision identification of different physiological stages, including barrier formation, maturation, injury, and recovery. This system possesses multi-position, non-invasive dynamic monitoring capabilities, and its measurements correlate strongly with changes in tight junction proteins as revealed by immunofluorescence staining. This technology provides a more powerful and reliable in vitro evaluation tool for drug delivery research and barrier-related pathology studies.

3 Imaging techniques for BBB permeability assessment

In vitro BBB models partly recapitulate the structure and function of the barrier, and corresponding permeability assessment in these models is essential for CNS research and early-stage drug screening. However, if subtle regional changes in BBB integrity need to be detected, multiple in vivo imaging techniques are required, such as computed tomography (CT), magnetic resonance imaging (MRI), positron emission tomography (PET), and optical imaging (Table 2). These methods can dynamically monitor changes in BBB permeability, molecular transport processes, and intercellular interactions, providing direct visual evidence for understanding the pathological mechanisms of CNS disorders and evaluating treatment efficacy.

3.1 MRI

3.1.1 Non-contrast MRI

Water molecules freely traverse the BBB and exhibit high sensitivity to early pathological changes in the BBB (Cornford and Hyman, 1999). As the main source of MRI signal, water provides sufficient sensitivity without exogenous contrast agents, making it an ideal endogenous tracer for assessing BBB function. Arterial spin labeling (ASL) is widely employed for the quantitative evaluation of cerebral perfusion and other hemodynamic parameters through the manipulation and modeling of the water signal in blood (St. Lawrence et al., 2000, 2012; Parkes and Tofts, 2002; Wang et al., 2007; Liu et al., 2011). Based on ASL, Lin et al. (2018) developed a non-contrast MRI technique that quantifies the water-extraction fraction and permeability parameters by detecting the signal from venous blood flowing into the superior sagittal sinus, which enables the quantitative assessment of BBB water permeability. Under mild hypercapnic conditions, this technique becomes much more sensitive, opening a new avenue for the non-invasive, safe monitoring of BBB function.

In recent years, this technique has shown promise in various neurological disease models. Mouchtouris

Table 2 In vivo imaging technologies for BBB assessment

Imaging technology	Application in BBB assessment	Sensitivity	Resolution	Penetration depth
MRI				
NC-MRI	Assessment of the BBB integrity through water MRI signals	Relatively low (based on water proton signal)	10–100 μm	
DCE-MRI	Evaluation of BBB leakage based on contrast agent (gadolinium) injection	Medium (dependent on contrast agent)	1–2 mm	
CT				
Conventional CT	Evaluation of the BBB permeability based on X-ray signal of contrast agents (iodine)	Relatively low (10^{-6} mol/L)	50 μm	
CTP	Quantitative assessment of BBB damage by analyzing the time–density curve of contrast agent	Moderate (dependent on iodine concentration)	0.5–1.0 mm	Equivalent to CT (limited by detector coverage)
Spectral CT	Precise analysis of BBB leakage of contrast agent based on X-ray energy spectrum	Higher for specific substances (iodine) than those of conventional CT	50–200 μm	
PET	Dynamic quantitative analysis of the BBB permeability of radionuclide-labeled substances (drug, protein, and peptide)	High (10^{-12}–10^{-11}mol/L)	1–2 mm	
FI				
NIR-II	Real-time, dynamic visualization of the entire process of BBB based on NIR-II fluorescence imaging	High (10^{-12}–10^{-9} mol/L)	2–3 mm (deep dependency)	3 cm
TPM	High-resolution assessment of molecular crossing of the BBB based on in vivo or cellular-level FI	High	Submicron scale (approximately 0.65 μm)	1 mm
PAI	A comprehensive assessment of BBB permeability by combining high-resolution vascular structure and function information obtained from fluorescence and ultrasound imaging	High	0.4–0.6 mm	Approximately 1 cm

BBB: blood–brain barrier; MRI: magnetic resonance imaging; CT: computed tomography; PET: positron emission tomography; FI: fluorescence imaging; PAI: photoacoustic imaging; NC-MRI: non-contrast MRI; DCE-MRI: dynamic contrast-enhanced MRI; CTP: CT perfusion; NIR-II: near-infrared II; TPM: two-photon microscopy.

et al. (2024) used non-contrast MRI to assess BBB permeability in patients with acute ischemic stroke. They employed a diffusion-prepared pseudo-continuous ASL (DP-pCASL) sequence to measure the water exchange rate and combined it with neurite orientation dispersion and density imaging (NODDI) sequence analysis to characterize tissue microstructure. The results revealed that the water exchange rate was correlated with post-stroke time and tissue parameters, and was also influenced by mechanical thrombectomy. Xiong et al. (2025) used the non-contrast MRI technique to conduct a longitudinal study in an AD mouse model. They found that as the disease progressed, both BBB water permeability and transmembrane water exchange in the hippocampal region were increased, accompanied by abnormal polarization of the AQP4 water channel protein. These impairments in key components of the glymphatic system are associated with the deposition of Aβ and Tau proteins, revealing the role of waste clearance failure in AD pathogenesis.

3.1.2 Dynamic contrast-enhanced MRI

Dynamic contrast-enhanced MRI (DCE-MRI) is another MRI method that requires intravenous injection of gadolinium-based contrast agents. Through repeated scanning, it captures signal changes caused by trans-BBB extravasation of contrast agents and quantifies its leakage rate, thereby assessing the degree of BBB opening. Over the past two decades, DCE-MRI

has become a well-established technique for evaluating BBB leakage in vivo (Heye et al., 2014; Raja et al., 2018).

DCE-MRI has been used to study cerebral small vessel disease (cSVD). Zhang et al. (2019) used a dual-temporal-resolution DCE-MRI protocol combined with the Patlak pharmacokinetic model, which quantified both the BBB leakage rate and leakage volume. Their results indicated that within white matter hyperintensity (WMH) regions of cSVD patients, the spatial extent of leakage was expanded, yet the leakage rate was reduced, suggesting a chronic, diffuse leakage process. In contrast, during healthy aging, the leakage rate was correlated with cognitive decline. Further elucidating this, Verstappen et al. (2025) utilized high-resolution DCE-MRI to reveal that BBB impairment in cSVD patients exhibits spatial heterogeneity: leakage was more pronounced in the normal-appearing white matter (NAWM) distal to WMH borders, forming a proximal-to-distal gradient pattern. Thus, BBB damage in cSVD is not uniform but is closely associated with microvascular architecture and local blood flow regulation. These findings provide crucial imaging evidence for understanding the spatial heterogeneity of BBB impairment and highlight the potential of BBB leakage as a biomarker for early diagnosis and therapeutic evaluation in cSVD.

DCE-MRI has also provided important evidence on BBB dysfunction in the early stages of AD. Van de Haar et al. (2016) found no significant difference in leakage rate between global NAWM and cortical gray matter (GA) in early AD patients. BBB dysfunction in early AD mainly appears as diffuse, widespread, subtle leakage rather than a marked local increase. This study indicates that widespread BBB disruption is a principal pathological feature of early AD. Nation et al. (2019) further investigated the relationship between BBB disruption and early cognitive impairment through a combined analysis of DCE-MRI and CSF biomarkers. Their results demonstrated that during the early stages of cognitive decline, the BBB exhibits significant leakage within the hippocampus and its subfields, independent of changes in Aβ and Tau pathology. Concurrently, elevated levels of soluble platelet-derived growth factor receptor β (sPDGFRβ) in the CSF also showed an association between BBB disruption and injury to cerebral capillary pericytes. Hence, BBB disruption is an independent biomarker for early cognitive impairment, highlighting the independent role of NVU dysfunction in the pathogenesis of AD and suggesting a new direction for early diagnosis and intervention.

Furthermore, DCE-MRI has been applied to psychiatric disorders. Shang et al. (2024) provided the first in vivo evidence of significantly elevated BBB permeability in emotion-related brain regions (olfactory cortex, caudate nucleus, and thalamus) of patients with major depressive disorder (MDD). Importantly, this increase in permeability was positively correlated with the severity of depressive symptoms, providing direct imaging evidence for BBB disruption in MDD pathophysiology.

In summary, DCE-MRI has become a valuable tool for quantifying BBB permeability in vivo, though the main challenge remains standardizing acquisition and analytical pipelines to enable robust multicenter comparisons. Key frontiers include defining the prognostic value of distinct leakage phenotypes and validating BBB permeability metrics as endpoints for interventional trials. Looking ahead, DCE-MRI holds substantial translational potential for guiding precision medicine, validating BBB integrity as a therapeutic target, and serving as a biomarker in early-phase clinical trials.

3.2 CT

CT imaging produces cross-sectional images based on the differential X-ray absorption by various tissues. In BBB permeability assessment, CT relies on iodinated contrast agents: an intact BBB prevents contrast agent extravasation, whereas BBB disruption allows leakage into the interstitium, resulting in localized hyperdensity on CT images, termed “contrast enhancement.” CT offers rapid scanning, widespread availability, and high sensitivity for detecting hemorrhage and calcification, making it suitable for initial screening in acute brain injury. However, its application in BBB research is limited by insufficient quantitative capability, low soft-tissue contrast, radiation exposure, and limited functional information (Pardridge, 2005). CT perfusion (CTP) imaging has advanced CT-based BBB research. This technique involves the rapid intravenous bolus administration of a contrast agent, followed by continuous dynamic scanning of a selected tissue plane to generate time–density curves. BBB permeability parameters are then calculated by applying pharmacokinetic models (Miles and Griffiths, 2003). For instance, Xu et al. (2017) used CTP to

demonstrate a significant increase in BBB permeability in the perihematomal region within 24–72 h following acute spontaneous basal ganglia hemorrhage, which correlated positively with both hematoma and perihematomal edema volumes. Furthermore, Chen XY et al. (2024) found that relative permeability parameters from CTP in hypoperfused regions could predict the risk of parenchymal hematoma after mechanical thrombectomy in ischemic stroke patients, with better predictive value than that of conventional imaging markers.

Spectral CT, another major technological advancement, works on the principle that different materials exhibit distinct X-ray attenuation characteristics at different energy levels. Performing scans with two different X-ray energy spectra simultaneously or in rapid succession enables material decomposition (Johnson et al., 2007; Siegel et al., 2016; Winklhofer et al., 2017). Spectral CT can generate iodine density maps and virtual non-contrast images, improving detection of subtle BBB leakage while reducing artifacts and contrast agent dosage (Grkovski et al., 2023b). Research by Grkovski et al. (2023a) demonstrated that this technique allows for clearer differentiation between ischemic tissue and normal brain parenchyma post-stroke, enabling more precise lesion characterization and quantitative assessment. Consequently, spectral CT provides a powerful imaging tool for the more accurate evaluation of BBB injury in stroke, with the potential to optimize clinical management and prognostic evaluation.

3.3 PET

PET, as a highly sensitive molecular imaging technique, enables in vivo, non-invasive assessment of BBB permeability by tracking radiolabeled tracers. It detects ligand concentrations in the picomolar to femtomolar levels and quantifies parameters such as the tracer uptake rate or permeability–surface area product (PS) at the BBB. This transcends simple qualitative assessments of "present or absent," enabling precise comparisons across individuals and time points, thereby providing objective metrics for monitoring disease progression or therapeutic response. Additionally, PET offers targeting specificity; by selecting different radiotracers, it can specifically investigate various BBB functions. PET has been widely used in neurodegenerative diseases, brain tumor imaging, and drug development.

Chen et al. (2017) developed a radiotracer (^{18}F-aluminum-NOTA-conjugated truncated Evans Blue (EB), namely [^{18}F] FAI-NEB) that rapidly binds to serum albumin and used dynamic PET to assess tumor vascular leakage via a simplified quantitative parameter (P_s), which correlated well with traditional EB extraction and DCE-MRI. In another study, Chung et al. (2025) used a non-invasive method that combined high temporal-resolution total-body PET imaging with kinetic modeling to quantitatively measure the PS of molecules at the BBB. Using multiple tracers (e.g., ^{18}F-fluorodeoxyglucose [FDG], ^{18}F-fluciclovine, and ^{11}C-butanol), they simultaneously estimated cerebral blood flow and the BBB transport rate constant K_1 in a single scan, from which the molecular PS was calculated. In studies of healthy aging and patients with metabolic dysfunction-associated steatohepatitis (MASH), they found that BBB permeability to FDG decreases with advancing age. Dai et al. (2025) designed a novel fluorescent probe based on a quinoline-malononitrile (QM) scaffold, which has the capabilities of near-infrared fluorescence (NIRF), MRI, and PET trimodal imaging. This probe can cross the BBB and specifically bind to cerebral Aβ plaques. In AD mice, it showed higher brain radioactive accumulation (AD 1.7 %ID/g vs. wild-type controls 0.9 %ID/g, where ID refers to the injected dose) and enabled dynamic metabolic monitoring. This work integrated NIRF, MRI, and PET imaging capabilities into a single molecular probe, providing a powerful multifunctional imaging tool for the early diagnosis of AD.

PET imaging has also been used to evaluate BBB modulation in AD mice. Li WJ et al. (2025) used focused ultrasound (FUS) to induce transient, reversible BBB opening, enhancing the cerebral delivery of the radiotracer [^{68}Ga] STZL4110 in AD mice and improving PET signal-to-noise ratio. These findings contribute to the development of novel strategies for optimizing brain-targeted drug delivery and pathological imaging. Toyohara (2016) has elucidated the fundamental principles of PET imaging for investigating P-gp function at the BBB. As a critical efflux transporter, P-gp directly modulates the permeation of pharmaceuticals and toxins into the CNS, thereby influencing therapeutic efficacy and toxicological profiles in CNS disorders (Juliano and Ling, 1976; Ambudkar et al., 1999). P-gp hyperfunction may contribute to multidrug resistance, while hypofunction potentially elevates neurotoxicity risks. These advancements

highlight the utility of P-gp PET imaging for mechanistic investigations and clinical pharmacokinetic guidance for conditions such as epilepsy and depression.

In summary, PET is evolving from a descriptive research tool into a quantitative platform for precision neurovascular medicine. Standardizing tracer protocols and simplifying complex kinetic models will support the early diagnosis of neurological disorders, drug delivery, and efficacy assessment.

3.4 Fluorescence imaging

Fluorescence imaging (FI), with its non-invasive nature, high sensitivity, superior spatiotemporal resolution, and real-time dynamic imaging capabilities, has become a key tool in biomedical research. It enables multidimensional visualization from molecular to in vivo levels. In preclinical investigations of BBB permeability, FI offers rapid, intuitive dynamic monitoring (Hong et al., 2017). Advances in super-resolution optical imaging instruments, in vivo imaging equipment, and imaging probes have broadened its use for dynamic BBB detection in living organisms and high-resolution imaging of in vitro BBB models or excised tissues.

3.4.1 Ex vivo brain tissue BBB FI

Ex vivo FI is a standard method for evaluating BBB permeability. It typically involves intravenous administration of fluorescent tracers such as fluorescein isothiocyanate (FITC)-dextran or EB, followed by transcranial perfusion, brain extraction, and confocal microscopy to visualize tracer distribution and extravasation. This approach clearly visualizes whether the tracer remains confined within the blood vessels or has extravasated into the perivascular parenchyma, enabling precise anatomical localization of leakage sites. Zhang et al. (2020) systematically evaluated electroacupuncture stimulation at specific frequencies (2/100 Hz) for its effect on rat BBB permeability using EB and 20 kDa FITC-dextran combined with confocal microscopy. The results demonstrated that electroacupuncture reversibly enhanced BBB permeability in rats, with restoration within 12 h post-stimulation. Imaging revealed tracer extravasation in the cerebral cortex and perivascular regions, indicating that electroacupuncture induces reversible BBB opening by modulating tight junction proteins (e.g., ZO-1 and occludin). Shumer-Elbaz et al. (2025) combined low-frequency FUS with microbubbles to deliver ionizable lipid nanoparticles (LNPs) to glioblastoma (GBM) regions. They assessed BBB opening by examining EB and fluorescent dextran extravasation in brain sections, and used cyanine 5 (Cy5)-labeled small interfering RNA (siRNA)-LNP fluorescence to confirm translocation and tumor accumulation. Confocal microscopy revealed the distribution of Cy5-siRNA-LNPs within tumor tissue, with co-localization in green fluorescent protein (GFP)-labeled tumor cells indicating cellular uptake. 4',6-Diamidino-2-phenylindole (DAPI) staining further illustrated the distribution of LNPs among non-tumor cells in the tumor microenvironment. This strategy overcomes the limitations of the BBB for LNP delivery, enabling LNP-based therapies for neurological disorders. Ex vivo imaging provides intuitive spatial localization and semi-quantitative data, but in vivo imaging technologies are needed for dynamic monitoring of BBB permeability.

3.4.2 In vivo FI techniques

In vivo FI techniques include wide-field, near-infrared I/II (NIR-I/II), and multiphoton FI. Conventional wide-field FI requires cranial window implantation or skull thinning (Yang et al., 2010; Wang et al., 2019) and offers limited resolution and depth, but is simple, cost-effective, compatible with diverse fluorescent probes, and suitable for large-scale screening and longitudinal studies. With advances in microscopy, NIR-I/II FI imaging has reduced tissue absorption and scattering of NIR light. NIR-II (1000–1700 nm) achieves approximately 3 cm depth, superior signal-to-noise ratio, and higher spatial resolution than visible or NIR-I (Hong et al., 2012; Cao et al., 2020). Wang et al. (2022) systematically modified aniline groups in dye molecules to create a series of NIR-II fluorophores with emission wavelengths ranging from 800 to 1400 nm. Certain dyes (e.g., BF_1 and BF_6) with molecular weights below 450 kDa cross the intact BBB for non-invasive, high-fidelity NIR-II FI of the mouse brain parenchyma. Lu et al. (2024) developed a novel NIR-II imaging probe (named DGC) that targets connective tissue growth factor (CTGF) for early AD detection. Comprising gold nanoclusters and cyclic peptides, DGC exhibits high BBB affinity (K_D= 21.9 nmol/L, where K_D is the dissociation equilibrium constant) and penetration ability, allowing clear visualization of elevated cerebral CTGF levels in 1-month-old amyloid precursor protein/presenilin 1 (APP/PS1) transgenic mice. Additionally, this probe supports

multimodal analysis, including FI, chromogenic reaction, and inductively coupled plasma mass spectrometry (ICP-MS) quantification, and has been validated in human AD brain sections. Notably, Zhang et al. (2023) conducted pioneering research that achieved real-time multiplexed NIR-II imaging enhanced by deep learning—a breakthrough marking a crucial step toward the clinical translation of biomedical optical imaging technologies. However, the practical application of this technology in assessing BBB permeability still faces several translational hurdles. These include reduced signal fidelity due to increased imaging depth, the lack of clinically validated BBB-specific tracers, and challenges related to the in vivo stability, biosafety, and scalable production of NIR-II imaging probes.

Multiphoton microscopy (MPM), particularly two-photon microscopy (TPM), uses NIR femtosecond laser pulses to enable real-time, label-free, subcellular resolution imaging of biological tissues with minimal photodamage—achieving depths of hundreds of micrometers, low phototoxicity, and rapid acquisition (Denk et al., 1990). In BBB research, TPM allows dynamic, real-time monitoring of leakage processes. Lee et al. (2018) used real-time in vivo two-photon imaging to study the effects of chronic restraint stress on the mouse cerebrovascular system. Their research revealed that chronic stress induced generalized vasoconstriction, reduced total cerebrovascular volume, and concomitant BBB hyperpermeability. These pathological changes were associated with upregulated cerebral vascular endothelial growth factor-A (VEGF-A) expression and downregulated tight junction protein Claudin-5. TPM also serves as a tool for evaluating the impact of pharmacological or physical interventions (e.g., FUS) on BBB permeability. Poon et al. (2018) investigated the effects of FUS combined with microbubbles on Aβ plaques in AD model mice. Using in vivo real-time two-photon imaging, they visualized immediate BBB opening post-FUS (evidenced by dextran leakage) and tracked individual Aβ plaques over time. The results indicated that a single FUS session simultaneously enhanced BBB permeability and reduced plaque volume by 62% within two days, persisting for two weeks, suggesting that FUS promotes Aβ clearance via transient BBB opening. Subsequent MRI-guided repeated FUS treatments confirmed the feasibility and cumulative efficacy of this protocol.

Although TPM offers unparalleled advantages in preclinical studies, its extremely shallow penetration depth and the need for craniotomy or the implantation of a transparent cranial window limit its clinical translation potential. Consequently, TPM is primarily used for basic research.

3.5 Photoacoustic imaging

Photoacoustic imaging (PAI) is an emerging non-invasive biomedical imaging modality that combines optical contrast with the ultrasonic penetration depth. It generates ultrasonic waves via thermoelastic expansion following light absorption in biological tissues, with signal amplitude reflecting local optical properties (Hui et al., 2016; Chen HY et al., 2024; Wang et al., 2024). Multiwavelength PAI enables high-contrast imaging of molecular targets at centimeter depth, overcoming the depth limits of conventional optical imaging (Liu XG et al., 2021; Lin and Wang, 2022).

The potential of PAI for assessing BBB integrity has been vividly demonstrated by recent studies utilizing novel molecular probes. Qin et al. (2025) developed a novel fluorescence/photoacoustic probe (namely, IVTPO) based on an electron donor-π-acceptor (D-π-A) system for GBM imaging. This probe exhibits strong optical absorption (572 nm), high molar extinction coefficient (12.29×10^4 $M^{-1}\cdot cm^{-1}$, where M represents mol/L), and outstanding BBB penetration. In GBM mouse models, IVTPO enabled real-time PAI through the intact skull, clearly delineating tumor location, abnormal vascular structures, and early probe extravasation in peritumoral regions. Compared to EB, IVTPO showed superior sensitivity and targeting, detecting subtle leakage before full BBB disruption, offering a powerful tool for early GBM diagnosis. Li J et al. (2025) reported a D-π-A molecular probe DMA-Te, which was constructed by chalcogenapyrylium modulation with *N*,*N*-dimethylaniline (DMA) as the donor and the chalcogenapyrylium moiety as the acceptor, for high-contrast PAI of Aβ plaques in AD. By incorporating a Te atom as an electron acceptor, this probe achieves a red-shifted absorption peak at 794 nm while maintaining a low fluorescence quantum yield (0.0006), favoring strong photoacoustic signal generation. The probe exhibits 20.8% BBB penetration rate and a high Aβ-binding affinity. In AD mice, a dual-wavelength PAI system successfully imaged Aβ plaques and cerebral vasculature simultaneously with high resolution.

Despite promising preclinical advances, the clinical translation of PAI faces dual challenges. First, the development of molecular probes is constrained by challenges in biocompatibility, pharmacokinetics, and scalable production. Probes such as IVTPO and DMA-Te, for instance, require extensive safety validation beyond rodent models. Second, the field lacks standardized quantitative methods, currently relying on descriptors such as "signal enhancement" rather than offering universally comparable, dynamic metrics of BBB permeability. Future efforts should focus on developing novel probes, establishing robust quantitative standards, and validating reliability through multicenter clinical studies.

4 Artificial intelligence in enhancing BBB permeability assessment

In vitro BBB models and in vivo imaging techniques remain essential tools for assessing BBB permeability, but they face challenges such as high costs, long time, and limited mechanistic insights. Artificial intelligence (AI) is reshaping the field by integrating multi-omics data, simulating molecule–barrier interactions, optimizing drug design workflows, and analyzing biomedical images (Clark, 2003; Saxena et al., 2019).

Currently, key AI approaches for predicting BBB permeability (Grant et al., 2025) include classical machine learning based on chemical descriptors (Yuan et al., 2018; Shaker et al., 2021), deep learning utilizing graph neural networks (Withnall et al., 2020; Jiang et al., 2021; Dey and Ning, 2024), and natural language processing based on simplified molecular input line entry system (SMILES) sequences (Tevosyan et al., 2022; Wen et al., 2022; Rollins et al., 2024). These models significantly accelerate drug development by predicting candidate permeability and elucidating BBB interactions. In particular, descriptor-based models offer a key advantage in their interpretability, providing mechanistic insights into prediction outcomes. For instance, Liu LL et al. (2021) employed support vector machine (SVM), random forest (RF), and extreme gradient boosting (XGBoost) algorithms with 1757 compounds and nine molecular fingerprints to construct an ensemble of 27 base classifiers, optimizing BBB permeability predictions. Their study calculated the average reduction in the Gini coefficient for molecular fingerprints using an RF model, enabling clear quantification of the contributions of different molecular substructures to prediction outcomes. It explicitly identified a strong correlation between oxygen-containing polar groups (e.g., carboxylic acids and polyhydroxy structures) and BBB impermeability. However, these models rely on predefined molecular descriptors and may overlook complex interactions. In contrast, deep learning with graph neural networks demonstrates significant potential by directly representing molecular structure and spatial information. For example, Group Graph is a novel substructure-level method that balances computational efficiency and representational capacity by simplifying graphs while preserving chemical information (Cao et al., 2024). However, this process simplifies stereochemical information and omits 3D structural details, which may limit its use in high-value contexts. Language-based BBB permeability prediction methods treat SMILES strings as textual input, enabling end-to-end learning without predefined features, making them suitable for large-scale pretraining. However, their performance typically lags behind that of traditional classical and graph-based models, and they suffer from poor interpretability. Molecular Prediction Model Fine-Tuning (MolPMoFiT) is a transfer learning approach pretrained on millions of compounds and fine-tuned on small datasets. It matches or surpasses state-of-the-art models for BBB permeability prediction, especially in data-sparse scenarios (Li and Fourches, 2020).

AI also aids in the quantitative analysis of biomedical images. Jackson et al. (2021) developed a novel computational tool for CNS PET tracer design using a dataset of 140 tracers. By analyzing seven physicochemical properties—including computed logarithm of the partition coefficient (clogP) and topological polar surface area (tPSA)—they identified differences between successful and non-penetrating tracers in tPSA and clogP. Their screening tool achieved 96.7% specificity and 97.4% positive predictive value, enabling early elimination of failures. This work provides valuable data and efficient computational tools to support the rational design of future CNS PET tracers. In a different application, Zhang et al. (2023) developed a novel method combining optical coherence tomography (OCT) with deep learning (pix2pix cGAN)

for rapid, non-invasive visualization and quantification of microvessels in 3D BBB models. By outperforming traditional morphological processing and RF methods, this deep learning approach achieves superior accuracy in segmenting vessels in low-contrast OCT images. It thus provides an efficient, label-free analytical tool for assessing permeability in BBB models and for drug screening applications.

5 Conclusions and future directions

In conclusion, precise assessment of BBB permeability is essential for understanding mechanisms of neurological disease and improving drug development. In vitro models serve as crucial screening platforms in early drug discovery, evolving from traditional static transwell systems to dynamic models that incorporate fluid shear stress (e.g., hollow-fiber reactors and microfluidic chips), and more recently, to highly biomimetic organoid models—progressively enhancing their capacity to replicate the complex microenvironment of NVU. The permeability of in vitro BBB models is evaluated by measuring P_{app} and TEER. At the in vivo level, imaging technologies complement one another to establish a comprehensive system for real-time, non-invasive assessment of BBB permeability.

To overcome the limitations of existing technologies in physiological relevance, dynamic monitoring capabilities, and quantitative accuracy, future BBB permeability assessment technologies will exhibit a distinct trend toward multimodal integration and intelligence-driven strategies. On the one hand, in vitro model systems will evolve from "simple simulation" to "precision recapitulation": patient-specific organ-on-a-chip and organoid technologies will achieve highly biomimetic reconstruction of NVU, closely mimicking the human physiological environment. The integration of high-throughput barrier assessment, transporter functional analysis, and multi-omics technologies will enable multidimensional characterization of functional phenotypes. On the other hand, in vivo imaging will use high-resolution MRI, novel PET probes, and NIR-II optical imaging to achieve non-invasive, dynamic, quantitative monitoring of BBB permeability.

AI will become the core driver of this paradigm. By integrating multi-omics data, simulating molecule–barrier interactions, and optimizing drug design, such as using deep learning to predict compound permeability or intelligently identifying barrier damage features from imaging data, AI will fundamentally reshape BBB permeability research. The deep integration of AI will establish a closed loop of "computational prediction–in vitro validation–in vivo confirmation," not only dramatically enhancing drug screening efficiency but also enabling the mechanistic interpretation and dynamic prediction of BBB function through multi-omics data integration. Furthermore, the deep application of AI in image processing will enable the automatic and quantitative extraction of critical information—such as leakage characteristics and vascular network morphology—from vast optical imaging datasets. This advancement will bridge the gap between mere observation and comprehensive understanding, as well as predictive capabilities. These developments will significantly enhance our ability to perform dynamic, holistic analyses of the functional state of the BBB in living organisms, ultimately driving innovation in diagnostic approaches and therapeutic strategies for CNS disorders.

Acknowledgments

This study was supported by the National Key Research and Development Program of China (No. 2023YFF0724100) and the National Natural Science Foundation of China (Nos. 22393934 and 22274097).

Author contributions

Yanhong SUN, Shihua LUO, Ying ZHU, and Miaomiao WANG conceived, designed, discussed the work, and revised the manuscript. Lu GAN, Miaomiao WANG, and Yiru FAN edited the manuscript. Miaomiao WANG and Chenxi DUAN prepared figures. All authors have read and approved the final manuscript, and therefore, have full access to all the data in the study and take responsibility for the integrity and security of the data.

Compliance with ethics guidelines

Miaomiao WANG, Lu GAN, Yiru FAN, Chenxi DUAN, Ying ZHU, Shihua LUO, and Yanhong SUN declare that they have no conflicts of interest.

This review does not contain any studies with human or animal subjects performed by any of the authors.

Declaration on the use of generative AI tools

In preparing this work, the authors used DeepSeek to refine language and grammar, and Doubao to improve artwork visual quality (e.g., resolution and color correction). The authors reviewed and edited the output and take full responsibility for the final content.

References

Ahlawat J, Barroso GG, Asil SM, et al., 2020. Nanocarriers as potential drug delivery candidates for overcoming the blood–brain barrier: challenges and possibilities. *ACS Omega*, 5(22):12583-12595. https://doi.org/10.1021/acsomega.0c01592

Ambudkar SV, Dey S, Hrycyna CA, et al., 1999. Biochemical, cellular, and pharmacological aspects of the multidrug transporter. *Annu Rev Pharmacol Toxicol*, 39: 361-398. https://doi.org/10.1146/annurev.pharmtox.39.1.361

Anderson JM, van Itallie CM, 2009. Physiology and function of the tight junction. *Cold Spring Harb Perspect Biol*, 1: a002584. https://doi.org/10.1101/cshperspect.a002584

Appelt-Menzel A, Cubukova A, Günther K, et al., 2017. Establishment of a human blood–brain barrier co-culture model mimicking the neurovascular unit using induced pluri- and multipotent stem cells. *Stem Cell Rep*, 8(4): 894-906. https://doi.org/10.1016/j.stemcr.2017.02.021

Badiola-Mateos M, di Giuseppe D, Paoli R, et al., 2021. A novel multi-frequency trans-endothelial electrical resistance (MTEER) sensor array to monitor blood–brain barrier integrity. *Sens Actuators B Chem*, 334:129599. https://doi.org/10.1016/j.snb.2021.129599

Bagchi S, Chhibber T, Lahooti B, et al., 2019. In-vitro blood–brain barrier models for drug screening and permeation studies: an overview. *Drug Des Devel Ther*, 13:3591-3605. https://doi.org/10.2147/dddt.s218708

Balzer V, Poc P, Puris E, et al., 2022. Re-evaluation of the hCMEC/D3 based in vitro BBB model for ABC transporter studies. *Eur J Pharm Biopharm*, 173:12-21. https://doi.org/10.1016/j.ejpb.2022.02.017

Banerjee J, Shi YJ, Azevedo HS, 2016. *In vitro* blood–brain barrier models for drug research: state-of-the-art and new perspectives on reconstituting these models on artificial basement membrane platforms. *Drug Discov Today*, 21(9): 1367-1386. https://doi.org/10.1016/j.drudis.2016.05.020

Banks WA, 2016. From blood–brain barrier to blood–brain interface: new opportunities for CNS drug delivery. *Nat Rev Drug Discov*, 15:275-292. https://doi.org/10.1038/nrd.2015.21

Bayir E, Celtikoglu MM, Sendemir A, 2019. The use of bacterial cellulose as a basement membrane improves the plausibility of the static *in vitro* blood–brain barrier model. *Int J Biol Macromol*, 126:1002-1013. https://doi.org/10.1016/j.ijbiomac.2018.12.257

Bell RD, Winkler EA, Sagare AP, et al., 2010. Pericytes control key neurovascular functions and neuronal phenotype in the adult brain and during brain aging. *Neuron*, 68(3): 409-427. https://doi.org/10.1016/j.neuron.2010.09.043

Benson K, Cramer S, Galla HJ, 2013. Impedance-based cell monitoring: barrier properties and beyond. *Fluids Barriers CNS*, 10:5. https://doi.org/10.1186/2045-8118-10-5

Bergmann S, Lawler SE, Qu Y, et al., 2018. Blood–brain-barrier organoids for investigating the permeability of CNS therapeutics. *Nat Protoc*, 13(12):2827-2843. https:/doi.org/10.1038/s41596-018-0066-x

Bhattacharya A, Kaushik DK, Lozinski BM, et al., 2020. Beyond barrier functions: roles of pericytes in homeostasis and regulation of neuroinflammation. *J Neurosci Res*, 98(12):2390-2405. https://doi.org/10.1002/jnr.24715

Cao J, Zhu BL, Zheng KF, et al., 2020. Recent progress in NIR-II contrast agent for biological imaging. *Front Bioeng Biotechnol*, 7:487. https://doi.org/10.3389/fbioe.2019.00487

Cao PY, He Y, Cui MY, et al., 2024. Group graph: a molecular graph representation with enhanced performance, efficiency and interpretability. *J Cheminform*, 16:133. https://doi.org/10.1186/s13321-024-00933-x

Ceccarelli MC, Lefevre MC, Marino A, et al., 2024. Real-time monitoring of a 3D blood–brain barrier model maturation and integrity with a sensorized microfluidic device. *Lab Chip*, 24(22):5085-5100. https://doi.org/10.1039/d4lc00633j

Cecchelli R, Berezowski V, Lundquist S, et al., 2007. Modelling of the blood–brain barrier in drug discovery and development. *Nat Rev Drug Discov*, 6:650-661. https://doi.org/10.1038/nrd2368

Chen HJ, Tong X, Lang LX, et al., 2017. Quantification of tumor vascular permeability and blood volume by positron emission tomography. *Theranostics*, 7(9):2363-2376. https://doi.org/10.7150/thno.19898

Chen HY, Mirg S, Gaddale P, et al., 2024. Multiparametric brain hemodynamics imaging using a combined ultrafast ultrasound and photoacoustic system. *Adv Sci*, 11(31): 2401467. https://doi.org/10.1002/advs.202401467

Chen XY, Xu J, Guo SY, et al., 2024. Blood–brain barrier permeability by CT perfusion predicts parenchymal hematoma after recanalization with thrombectomy. *J Neuroimaging*, 34(2):241-248. https://doi.org/10.1111/jon.13172

Chung B, Kim J, Nam J, et al., 2020. Evaluation of cell-penetrating peptides using microfluidic in vitro 3D brain endothelial barrier. *Macromol Biosci*, 20(6):1900425. https://doi.org/10.1002/mabi.201900425

Chung KJ, Abdelhafez YG, Spencer BA, et al., 2025. Quantitative PET imaging and modeling of molecular blood–brain barrier permeability. *Nat Commun*, 16:3076. https://doi.org/10.1038/s41467-025-58356-7

Clark DE, 2003. *In silico* prediction of blood–brain barrier permeation. *Drug Discov Today*, 8(20):927-933. https://doi.org/10.1016/S1359-6446(03)02827-7

Cornford EM, Hyman S, 1999. Blood–brain barrier permeability to small and large molecules. *Adv Drug Deliv Rev*, 36(2-3):145-163. https://doi.org/10.1016/S0169-409X(98)00082-9

Cucullo L, Couraud PO, Weksler B, et al., 2008. Immortalized human brain endothelial cells and flow-based vascular modeling: a marriage of convenience for rational neurovascular studies. *J Cereb Blood Flow Metab*, 28(2): 312-328.
https://doi.org/10.1038/sj.jcbfm.9600525

Cucullo L, Marchi N, Hossain M, et al., 2011. A dynamic *in vitro* BBB model for the study of immune cell trafficking into the central nervous system. *J Cereb Blood Flow Metab*, 31(2):767-777.
https://doi.org/10.1038/jcbfm.2010.162

Dai JF, Wei WJ, Yan CX, et al., 2025. Multiplex imaging of amyloid-β plaques dynamics in living brains with quinoline-malononitrile-based probes. *Nat Biomed Eng*, 9:1632-1644.
https://doi.org/10.1038/s41551-025-01392-x

Daniels BP, Cruz-Orengo L, Pasieka TJ, et al., 2013. Immortalized human cerebral microvascular endothelial cells maintain the properties of primary cells in an *in vitro* model of immune migration across the blood brain barrier. *J Neurosci Methods*, 212(1):173-179.
https://doi.org/10.1016/j.jneumeth.2012.10.001

Dao L, You Z, Lu L, et al., 2024. Modeling blood–brain barrier formation and cerebral cavernous malformations in human PSC-derived organoids. *Cell Stem Cell*, 31(6): 818-833.e11.
https://doi.org/10.1016/j.stem.2024.04.019

de Vivo DC, Trifiletti RR, Jacobson RI, et al., 1991. Defective glucose transport across the blood–brain barrier as a cause of persistent hypoglycorrhachia, seizures, and developmental delay. *N Engl J Med*, 325(10):703-709.
https://doi.org/10.1056/nejm199109053251006

Deli MA, Ábrahám CS, Kataoka Y, et al., 2005. Permeability studies on in vitro blood–brain barrier models: physiology, pathology, and pharmacology. *Cell Mol Neurobiol*, 25: 59-127.
https://doi.org/10.1007/s10571-004-1377-8

Denk W, Strickler JH, Webb WW, 1990. Two-photon laser scanning fluorescence microscopy. *Science*, 248:73-76.
https://doi.org/10.1126/science.2321027

Dey V, Ning X, 2024. Enhancing molecular property prediction with auxiliary learning and task-specific adaptation. *J Cheminform*, 16:85.
https://doi.org/10.1186/s13321-024-00880-7

Dohgu S, Takata F, Yamauchi A, et al., 2005. Brain pericytes contribute to the induction and up-regulation of blood–brain barrier functions through transforming growth factor-β production. *Brain Res*, 1038(2):208-215.
https://doi.org/10.1016/j.brainres.2005.01.027

Dong XW, 2018. Current strategies for brain drug delivery. *Theranostics*, 8(6):1481-1493.
https://doi.org/10.7150/thno.21254

Douville NJ, Tung YC, Li R, et al., 2010. Fabrication of two-layered channel system with embedded electrodes to measure resistance across epithelial and endothelial barriers. *Anal Chem*, 82(6):2505-2511.
https://doi.org/10.1021/ac9029345

Fernández-Seara MA, Wang Z, Wang JJ, et al., 2005. Continuous arterial spin labeling perfusion measurements using single shot 3D GRASE at 3 T. *Magn Reson Med*, 54(5): 1241-1247.
https://doi.org/10.1002/mrm.20674

Franke H, Galla HJ, Beuckmann CT, 1999. An improved low-permeability in vitro-model of the blood–brain barrier: transport studies on retinoids, sucrose, haloperidol, caffeine and mannitol. *Brain Res*, 818(1):65-71.
https://doi.org/10.1016/S0006-8993(98)01282-7

Grant N, Machado Reyes D, Yang ZF, et al., 2025. Blood brain barrier permeability prediction with artificial intelligence and machine learning: a meta-review and future directions. *Discov Artif Intell*, 5:254.
https://doi.org/10.1007/s44163-025-00494-4

Grkovski R, Acu L, Ahmadli U, et al., 2023a. A novel dual-energy CT method for detection and differentiation of intracerebral hemorrhage from contrast extravasation in stroke patients after endovascular thrombectomy: feasibility and first results. *Clin Neuroradiol*, 33:171-177.
https://doi.org/10.1007/s00062-022-01198-3

Grkovski R, Acu L, Ahmadli U, et al., 2023b. Dual-energy computed tomography in stroke imaging: value of a new image acquisition technique for ischemia detection after mechanical thrombectomy. *Clin Neuroradiol*, 33: 747-754.
https://doi.org/10.1007/s00062-023-01270-6

Hajal C, Offeddu GS, Shin Y, et al., 2022. Engineered human blood–brain barrier microfluidic model for vascular permeability analyses. *Nat Protoc*, 17:95-128.
https://doi.org/10.1038/s41596-021-00635-w

Harilal S, Jose J, Parambi DGT, et al., 2020. Revisiting the blood–brain barrier: a hard nut to crack in the transportation of drug molecules. *Brain Res Bull*, 160:121-140.
https://doi.org/10.1016/j.brainresbull.2020.03.018

He QG, Liu J, Liang J, et al., 2018. Towards improvements for penetrating the blood-brain barrier—recent progress from a material and pharmaceutical perspective. *Cells*, 7(4):24.
https://doi.org/10.3390/cells7040024

Heye AK, Culling RD, Hernández MDCV, et al., 2014. Assessment of blood–brain barrier disruption using dynamic contrast-enhanced MRI. A systematic review. *Neuroimage Clin*, 6:262-274.
https://doi.org/10.1016/j.nicl.2014.09.002

Hong GS, Lee JC, Robinson JT, et al., 2012. Multifunctional *in vivo* vascular imaging using near-infrared II fluorescence. *Nat Med*, 18:1841-1846.
https://doi.org/10.1038/nm.2995

Hong GS, Antaris AL, Dai HJ, 2017. Near-infrared fluorophores for biomedical imaging. *Nat Biomed Eng*, 1:0010.
https://doi.org/10.1038/s41551-016-0010

Hui J, Li R, Phillips EH, et al., 2016. Bond-selective photoacoustic imaging by converting molecular vibration into acoustic waves. *Photoacoustics*, 4:11-21.
https://doi.org/10.1016/j.pacs.2016.01.002

Hurst RD, Fritz IB, 1996. Properties of an immortalised

vascular endothelial/glioma cell co-culture model of the blood–brain barrier. *J Cell Physiol*, 167:81-88. https://doi.org/10.1002/(SICI)1097-4652(199604)167:1<81::AID-JCP9>3.0.CO;2-8

Iliff JJ, Wang MH, Liao YH, et al., 2012. A paravascular pathway facilitates CSF flow through the brain parenchyma and the clearance of interstitial solutes, including amyloid β. *Sci Transl Med*, 4:147ra111. https://doi.org/10.1126/scitranslmed.3003748

Ito R, Umehara K, Suzuki S, et al., 2019. A human immortalized cell-based blood–brain barrier triculture model: development and characterization as a promising tool for drug–brain permeability studies. *Mol Pharm*, 16(11): 4461-4471. https://doi.org/10.1021/acs.molpharmaceut.9b00519

Jackson I, Luo A, Webb E, et al., 2021. A new *in silico* approach to revolutionize CNS PET tracer design and enhance translational success. *Nucl Med Biol*, 96-97:S24-S25. https://doi.org/10.1016/S0969-8051(21)00304-8

Janigro D, Leaman SM, Stanness KA, 1999. Dynamic in vitro modeling of the blood–brain barrier: a novel tool for studies of drug delivery to the brain. *Pharm Sci Technol Today*, 2:7-12. https://doi.org/10.1016/s1461-5347(98)00110-2

Jiang DJ, Wu ZX, Hsieh CY, et al., 2021. Could graph neural networks learn better molecular representation for drug discovery? A comparison study of descriptor-based and graph-based models. *J Cheminform*, 13:12. https://doi.org/10.1186/s13321-020-00479-8

Jiang LL, Li S, Zheng JS, et al., 2019. Recent progress in microfluidic models of the blood–brain barrier. *Micromachines*, 10(6):375. https://doi.org/10.3390/mi10060375

Johnson TRC, Krauß B, Sedlmair M, et al., 2007. Material differentiation by dual energy CT: initial experience. *Eur Radiol*, 17(6):1510-1517. https://doi.org/10.1007/s00330-006-0517-6

Juliano RL, Ling V, 1976. A surface glycoprotein modulating drug permeability in Chinese hamster ovary cell mutants. *Biochim Biophys Acta (BBA)-Biomembr*, 455:152-162. https://doi.org/10.1016/0005-2736(76)90160-7

Kadry H, Noorani B, Cucullo L, 2020. A blood–brain barrier overview on structure, function, impairment, and biomarkers of integrity. *Fluids Barriers CNS*, 17:69. https://doi.org/10.1186/s12987-020-00230-3

Kisler K, Nelson AR, Rege SV, et al., 2017. Pericyte degeneration leads to neurovascular uncoupling and limits oxygen supply to brain. *Nat Neurosci*, 20:406-416. https://doi.org/10.1038/nn.4489

Krol S, Macrez R, Docagne F, et al., 2013. Therapeutic benefits from nanoparticles: the potential significance of nanoscience in diseases with compromise to the blood brain barrier. *Chem Rev*, 113(3):1877-1903. https://doi.org/10.1021/cr200472g

Lee S, Kang BM, Kim JH, et al., 2018. Real-time *in vivo* two-photon imaging study reveals decreased cerebro-vascular volume and increased blood–brain barrier permeability in chronically stressed mice. *Sci Rep*, 8:13064. https://doi.org/10.1038/s41598-018-30875-y

Li J, Wang TT, Zhang X, et al., 2025. Chalcogenapyrylium-engineered D-π-A probe for enhanced optoacoustic imaging of amyloid-β plaques. *Sens Actuators B Chem*, 442:138086. https://doi.org/10.1016/j.snb.2025.138086

Li WJ, Zha XC, Zhang XY, et al., 2025. Enhanced positron emission tomography imaging of β-amyloid through focused ultrasound-mediated gallium-68 radiotracer delivery across the blood–brain barrier. *ACS Chem Neurosci*, 16(15):3070-3081. https://doi.org/10.1021/acschemneuro.5c00476

Li XH, Fourches D, 2020. Inductive transfer learning for molecular activity prediction: Next-Gen QSAR Models with MolPMoFiT. *J Cheminform*, 12:27. https://doi.org/10.1186/s13321-020-00430-x

Lin L, Wang LV, 2022. The emerging role of photoacoustic imaging in clinical oncology. *Nat Rev Clin Oncol*, 19: 365-384. https://doi.org/10.1038/s41571-022-00615-3

Lin ZX, Li Y, Su P, et al., 2018. Non-contrast MR imaging of blood–brain barrier permeability to water. *Magn Reson Med*, 80(4):1507-1520. https://doi.org/10.1002/mrm.271411

Liu JJ, Wang T, Dong J, et al., 2025. The blood-brain barriers: novel nanocarriers for central nervous system diseases. *J Nanobiotechnol*, 23:146. https://doi.org/10.1186/s12951-025-03247-8

Liu LL, Zhang L, Feng HW, et al., 2021. Prediction of the blood–brain barrier (BBB) permeability of chemicals based on machine-learning and ensemble methods. *Chem Res Toxicol*, 34(6):1456-1467. https://doi.org/10.1021/acs.chemrestox.0c00343

Liu PY, Uh J, Lu HZ, 2011. Determination of spin compartment in arterial spin labeling MRI. *Magn Reson Med*, 65(1):120-127. https://doi.org/10.1002/mrm.22601

Liu XG, Duan YK, Liu B, 2021. Nanoparticles as contrast agents for photoacoustic brain imaging. *Aggregate*, 2:4-19. https://doi.org/10.1002/agt2.26

Logan S, Arzua T, Canfield SG, et al., 2019. Studying human neurological disorders using induced pluripotent stem cells: from 2D monolayer to 3D organoid and blood brain barrier models. *Compr Physiol*, 9(2):565-611. https://doi.org/10.1002/j.2040-4603.2019.tb00076.x

Lu C, Meng C, Li YY, et al., 2024. A probe for NIR-II imaging and multimodal analysis of early Alzheimer's disease by targeting CTGF. *Nat Commun*, 15:5000. https://doi.org/10.1038/s41467-024-49409-4

Luissint AC, Artus C, Glacial F, et al., 2012. Tight junctions at the blood brain barrier: physiological architecture and disease-associated dysregulation. *Fluids Barriers CNS*, 9:23. https://doi.org/10.1186/2045-8118-9-23

Malik M, Steele SA, Mitra D, et al., 2025. Trans-epithelial/

endothelial electrical resistance (TEER): current state of integrated TEER measurements in organ-on-a-chip devices. *Curr Opin Biomed Eng*, 34:100588. https://doi.org/10.1016/j.cobme.2025.100588

Malinova TS, Huveneers S, 2018. Sensing of cytoskeletal forces by asymmetric adherens junctions. *Trends Cell Biol*, 28(4):328-341. https://doi.org/10.1016/j.tcb.2017.11.002

Mantecón-Oria M, Diban N, Berciano MT, et al., 2020. Hollow fiber membranes of PCL and PCL/graphene as scaffolds with potential to develop in vitro blood–brain barrier models. *Membranes*, 10(8):161. https://doi.org/10.3390/membranes10080161

Mantecón-Oria M, Tapia O, Lafarga M, et al., 2022a. Influence of the properties of different graphene-based nanomaterials dispersed in polycaprolactone membranes on astrocytic differentiation. *Sci Rep*, 12:13408. https://doi.org/10.1038/s41598-022-17697-9

Mantecón-Oria M, Rivero MJ, Diban N, et al., 2022b. On the quest of reliable 3D dynamic *in vitro* blood–brain barrier models using polymer hollow fiber membranes: pitfalls, progress, and future perspectives. *Front Bioeng Biotechnol*, 10:1056162. https://doi.org/10.3389/fbioe.2022.1056162

Mantecón-Oria M, Rivero MJ, Löscher W, et al., 2025. Breaking optical barriers: transparent polymeric hollow fibers for biomedical applications. *View*, 6(6):20250076. https://doi.org/10.1002/VIW.20250076

Mármol I, Abizanda-Campo S, Ayuso JM, et al., 2023. Towards novel biomimetic in vitro models of the blood–brain barrier for drug permeability evaluation. *Bioengineering*, 10(5):572. https://doi.org/10.3390/bioengineering10050572

Miles KA, Griffiths MR, 2003. Perfusion CT: a worthwhile enhancement? *Br J Radiol*, 76:220-231. https://doi.org/10.1259/bjr/13564625

Mouchtouris N, Ailes I, Gooch R, et al., 2024. Quantifying blood–brain barrier permeability in patients with ischemic stroke using non-contrast MRI. *Magn Reson Imaging*, 109:165-172. https://doi.org/10.1016/j.mri.2024.03.027

Muruganandam A, Herx LM, Monette R, et al., 1997. Development of immortalized human cerebromicrovascular endothelial cell line as an in vitro model of the human blood–brain barrier. *FASEB J*, 11(13):1187-1197. https://doi.org/10.1096/fasebj.11.13.9367354

Naik P, Cucullo L, 2012. *In vitro* blood–brain barrier models: current and perspective technologies. *J Pharm Sci*, 101(4): 1337-1354. https://doi.org/10.1002/jps.23022

Nakagawa S, Deli MA, Kawaguchi H, et al., 2009. A new blood–brain barrier model using primary rat brain endothelial cells, pericytes and astrocytes. *Neurochem Int*, 54(3-4):253-263. https://doi.org/10.1016/j.neuint.2008.12.002

Nation DA, Sweeney MD, Montagne A, et al., 2019. Blood–brain barrier breakdown is an early biomarker of human cognitive dysfunction. *Nat Med*, 25:270-276. https://doi.org/10.1038/s41591-018-0297-y

Nazari H, Shrestha J, Naei VY, et al., 2023. Advances in TEER measurements of biological barriers in microphysiological systems. *Biosens Bioelectron*, 234:115355. https://doi.org/10.1016/j.bios.2023.115355

Neuhaus W, Lauer R, Oelzant S, et al., 2006. A novel flow based hollow-fiber blood–brain barrier in vitro model with immortalised cell line *PBMEC/C1-2*. *J Biotechnol*, 125(1):127-141. https://doi.org/10.1016/j.jbiotec.2006.02.019

Nogueira DES, Cabral JMS, Rodrigues CAV, 2021. Single-use bioreactors for human pluripotent and adult stem cells: towards regenerative medicine applications. *Bioengineering*, 8(5):68. https://doi.org/10.3390/bioengineering8050068

Nzou G, Wicks RT, Wicks EE, et al., 2018. Human cortex spheroid with a functional blood brain barrier for high-throughput neurotoxicity screening and disease modeling. *Sci Rep*, 8:7413. https://doi.org/10.1038/s41598-018-25603-5

Oddo A, Peng B, Tong ZQ, et al., 2019. Advances in microfluidic blood–brain barrier (BBB) models. *Trends Biotechnol*, 37(12):1295-1314. https://doi.org/10.1016/j.tibtech.2019.04.006

Pandit R, Chen LY, Götz J, 2020. The blood–brain barrier: physiology and strategies for drug delivery. *Adv Drug Deliv Rev*, 165-166:1-14. https://doi.org/10.1016/j.addr.2019.11.009

Pardridge WM, 2005. The blood–brain barrier: bottleneck in brain drug development. *NeuroRx*, 2:3-14. https://doi.org/10.1602/neurorx.2.1.3

Parkes LM, Tofts PS, 2002. Improved accuracy of human cerebral blood perfusion measurements using arterial spin labeling: accounting for capillary water permeability. *Magn Reson Med*, 48(1):27-41. https://doi.org/10.1002/mrm.10180

Poon CT, Shah K, Lin C, et al., 2018. Time course of focused ultrasound effects on β-amyloid plaque pathology in the TgCRND8 mouse model of Alzheimer's disease. *Sci Rep*, 8:14061. https://doi.org/10.1038/s41598-018-32250-3

Qin W, Li HH, Chen JL, et al., 2025. Amphiphilic hemicyanine molecular probes crossing the blood-brain barrier for intracranial optical imaging of glioblastoma. *Sci Adv*, 11:eadq5816. https://doi.org/10.1126/sciadv.adq5816

Raja R, Rosenberg GA, Caprihan A, 2018. MRI measurements of blood–brain barrier function in dementia: a review of recent studies. *Neuropharmacology*, 134:259-271. https://doi.org/10.1016/j.neuropharm.2017.10.034

Rollins ZA, Cheng AC, Metwally E, 2024. MolPROP: molecular property prediction with multimodal language and graph fusion. *J Cheminform*, 16:56. https://doi.org/10.1186/s13321-024-00846-9

Rubin LL, Hall DE, Porter S, et al., 1991. A cell culture model of the blood–brain barrier. *J Cell Biol*, 115(6):1725-1735. https://doi.org/10.1083/jcb.115.6.1725

Saxena D, Sharma A, Siddiqui MH, et al., 2019. Blood brain barrier permeability prediction using machine learning techniques: an update. *Curr Pharm Biotechnol*, 20(14): 1163-1171. https://doi.org/10.2174/1389201020666190821145346

Schurhoff N, Toborek M, 2023. Circadian rhythms in the blood–brain barrier: impact on neurological disorders and stress responses. *Mol Brain*, 16:5. https://doi.org/10.1186/s13041-023-00997-0

Segarra M, Aburto MR, Acker-Palmer A, 2021. Blood–brain barrier dynamics to maintain brain homeostasis. *Trends Neurosci*, 44(5):393-405. https://doi.org/10.1016/j.tins.2020.12.002

Shaker B, Yu MS, Song JS, et al., 2021. LightBBB: computational prediction model of blood–brain-barrier penetration based on LightGBM. *Bioinformatics*, 37(8):1135-1139. https://doi.org/10.1093/bioinformatics/btaa918

Shang BL, Wang T, Zhao SL, et al., 2024. Higher blood–brain barrier permeability in patients with major depressive disorder identified by DCE-MRI imaging. *Psychiatry Res Neuroimaging*, 337:111761. https://doi.org/10.1016/j.pscychresns.2023.111761

Shumer-Elbaz M, Ad-El N, Chulanova Y, et al., 2025. Low-frequency ultrasound-mediated blood–brain barrier opening enables non-invasive lipid nanoparticle RNA delivery to glioblastoma. *J Control Release*, 385:114018. https://doi.org/10.1016/j.jconrel.2025.114018

Siegel MJ, Kaza RK, Bolus DN, et al., 2016. White paper of the Society of Computed Body Tomography and magnetic resonance on dual-energy CT, Part 1: technology and terminology. *J Comput Assist Tomogr*, 40(6):841-845. https://doi.org/10.1097/rct.0000000000000531

Simonneau C, Duschmalé M, Gavrilov A, et al., 2021. Investigating receptor-mediated antibody transcytosis using blood–brain barrier organoid arrays. *Fluids Barriers CNS*, 18:43. https://doi.org/10.1186/s12987-021-00276-x

Sivandzade F, Cucullo L, 2018. In-vitro blood–brain barrier modeling: a review of modern and fast-advancing technologies. *J Cereb Blood Flow Metab*, 38(10):1667-1681. https://doi.org/10.1177/0271678x18788769

Sonninen TM, Peltonen S, Kälvälä S, et al., 2025. From inserts to chips: microfluidic culture and 3D astrocyte co-culture drive functional and transcriptomic changes in hiPSC-derived endothelial cells. *Fluids Barriers CNS*, 22:58. https://doi.org/10.1186/s12987-025-00672-7

Srinivasan B, Kolli AR, Esch MB, et al., 2015. TEER measurement techniques for in vitro barrier model systems. *J Lab Autom*, 20(2):107-126. https://doi.org/10.1177/2211068214561025

St. Lawrence KS, Frank JA, McLaughlin AC, 2000. Effect of restricted water exchange on cerebral blood flow values calculated with arterial spin tagging: a theoretical investigation. *Magn Reson Med*, 44(3):440-449. https://doi.org/10.1002/1522-2594(200009)44:3<440::AID-MRM15>3.0.CO;2-6

St. Lawrence KS, Owen D, Wang DJJ, 2012. A two-stage approach for measuring vascular water exchange and arterial transit time by diffusion-weighted perfusion MRI. *Magn Reson Med*, 67(5):1275-1284. https://doi.org/10.1002/mrm.23104

Stamatovic SM, Johnson AM, Keep RF, et al., 2016. Junctional proteins of the blood–brain barrier: new insights into function and dysfunction. *Tissue Barriers*, 4(1):e1154641. https://doi.org/10.1080/21688370.2016.1154641

Stanness KA, Westrum LE, Fornaciari E, et al., 1997. Morphological and functional characterization of an in vitro blood–brain barrier model. *Brain Res*, 771(2):329-342. https://doi.org/10.1016/S0006-8993(97)00829-9

Sun JD, Song S, 2024. Advances in modeling permeability and selectivity of the blood–brain barrier using microfluidics. *Microfluid Nanofluidics*, 28(7):44. https://doi.org/10.1007/s10404-024-02741-z

Tevosyan A, Khondkaryan L, Khachatrian H, et al., 2022. Improving VAE based molecular representations for compound property prediction. *J Cheminform*, 14:69. https://doi.org/10.1186/s13321-022-00648-x

Toyohara J, 2016. Importance of P-gp PET imaging in pharmacology. *Curr Pharm Des*, 22(38):5830-5836. https://doi.org/10.2174/1381612822666160804092258

Turowski P, Kenny BA, 2015. The blood–brain barrier and methamphetamine: open sesame? *Front Neurosci*, 9:156. https://doi.org/10.3389/fnins.2015.00156

van de Haar HJ, Burgmans S, Jansen JFA, et al., 2016. Blood–brain barrier leakage in patients with early Alzheimer disease. *Radiology*, 281(2):527-535. https://doi.org/10.1148/radiol.2016152244

van der Helm MW, Odijk M, Frimat JP, et al., 2016. Direct quantification of transendothelial electrical resistance in organs-on-chips. *Biosens Bioelectron*, 85:924-929. https://doi.org/10.1016/j.bios.2016.06.014

Verstappen D, de Jong JJA, Voorter PHM, et al., 2025. DCE-MRI reveals spatial pattern in heterogeneous blood–brain barrier leakage within white matter in cerebral small vessel disease. *J Cereb Blood Flow Metab*, 45(11):2104-2114. https://doi.org/10.1177/0271678x251364151

Vorbrodt AW, Dobrogowska DH, 2003. Molecular anatomy of intercellular junctions in brain endothelial and epithelial barriers: electron microscopist's view. *Brain Res Rev*, 42(3):221-242. https://doi.org/10.1016/S0165-0173(03)00177-2

Wang D, Chen FL, Han ZL, et al., 2021. Relationship between amyloid-β deposition and blood–brain barrier dysfunction in Alzheimer's disease. *Front Cell Neurosci*, 15: 695479. https://doi.org/10.3389/fncel.2021.695479

Wang GX, Zhou YY, Yu CH, et al., 2024. Intravital photoacoustic brain stimulation with high-precision. *J Biomed Opt*, 29(S1):S11520. https://doi.org/10.1117/1.jbo.29.s1.s11520

Wang JJ, Fernández-Seara MA, Wang SM, et al., 2007. When

perfusion meets diffusion: in vivo measurement of water permeability in human brain. *J Cereb Blood Flow Metab*, 27(4):839-849. https://doi.org/10.1038/sj.jcbfm.9600398

Wang SC, Shi H, Wang LS, et al., 2022. Photostable small-molecule NIR-II fluorescent scaffolds that cross the blood–brain barrier for noninvasive brain imaging. *J Am Chem Soc*, 144(51):23668-23676. https://doi.org/10.1021/jacs.2c11223

Wang X, Li P, Ding Q, et al., 2019. Observation of acetylcholinesterase in stress-induced depression phenotypes by two-photon fluorescence imaging in the mouse brain. *J Am Chem Soc*, 141(5):2061-2068. https://doi.org/10.1021/jacs.8b11414

Wang XB, Hou Y, Ai XP, et al., 2020. Potential applications of microfluidics based blood brain barrier (BBB)-on-chips for in vitro drug development. *Biomed Pharmacother*, 132:110822. https://doi.org/10.1016/j.biopha.2020.110822

Weksler B, Romero IA, Couraud PO, 2013. The hCMEC/D3 cell line as a model of the human blood brain barrier. *Fluids Barriers CNS*, 10:16. https://doi.org/10.1186/2045-8118-10-16

Wen NF, Liu GQ, Zhang J, et al., 2022. A fingerprints based molecular property prediction method using the BERT model. *J Cheminform*, 14:71. https://doi.org/10.1186/s13321-022-00650-3

Wevers NR, Kasi DG, Gray T, et al., 2018. A perfused human blood–brain barrier on-a-chip for high-throughput assessment of barrier function and antibody transport. *Fluids Barriers CNS*, 15:23. https://doi.org/10.1186/s12987-018-0108-3

Winklhofer S, de Martini IV, Nern C, et al., 2017. Dual-energy computed tomography in stroke imaging: technical and clinical considerations of virtual noncontrast images for detection of the hyperdense artery sign. *J Comput Assist Tomogr*, 41(6):843-848. https://doi.org/10.1097/rct.0000000000000638

Withnall M, Lindelöf E, Engkvist O, et al., 2020. Building attention and edge message passing neural networks for bioactivity and physical-chemical property prediction. *J Cheminf*, 12:1. https://doi.org/10.1186/s13321-019-0407-y

Wu D, Chen Q, Chen XJ, et al., 2023. The blood–brain barrier: structure, regulation and drug delivery. *Signal Transduct Target Ther*, 8:217. https://doi.org/10.1038/s41392-023-01481-w

Xiong CH, Yu ZY, Yin Y, et al., 2025. Longitudinal changes of blood–brain barrier and transcytolemmal water exchange permeability in Alzheimer's disease mice: a non-contrast MRI study. *Neuroimage*, 310:121141. https://doi.org/10.1016/j.neuroimage.2025.121141

Xu HL, Li R, Duan YX, et al., 2017. Quantitative assessment on blood–brain barrier permeability of acute spontaneous intracerebral hemorrhage in basal ganglia: a CT perfusion study. *Neuroradiology*, 59(7):677-684. https://doi.org/10.1007/s00234-017-1852-9

Yang G, Pan F, Parkhurst CN, et al., 2010. Thinned-skull cranial window technique for long-term imaging of the cortex in live mice. *Nat Protoc*, 5:201-208. https://doi.org/10.1038/nprot.2009.222

Yang JY, Shin DS, Jeong M, et al., 2024. Evaluation of drug blood–brain-barrier permeability using a microfluidic chip. *Pharmaceutics*, 16(5):574. https://doi.org/10.3390/pharmaceutics16050574

Yang XY, Wang QZ, Cao EH, 2020. Structure of the human cation-chloride cotransporter NKCC1 determined by single-particle electron cryo-microscopy. *Nat Commun*, 11:1016. https://doi.org/10.1038/S41467-020-14790-3

Yuan YX, Zheng F, Zhan CG, 2018. Improved prediction of blood–brain barrier permeability through machine learning with combined use of molecular property-based descriptors and fingerprints. *AAPS J*, 20(3):54. https://doi.org/10.1208/s12248-018-0215-8

Zhang CE, Wong SM, Uiterwijk R, et al., 2019. Blood–brain barrier leakage in relation to white matter hyperintensity volume and cognition in small vessel disease and normal aging. *Brain Imaging Behav*, 13(2):389-395. https://doi.org/10.1007/s11682-018-9855-7

Zhang HT, Kang DH, Piantino M, et al., 2023. Rapid quantification of microvessels of three-dimensional blood–brain barrier model using optical coherence tomography and deep learning algorithm. *Biosensors*, 13(8):818. https://doi.org/10.3390/bios13080818

Zhang SS, Gong P, Zhang JS, et al., 2020. Specific frequency electroacupuncture stimulation transiently enhances the permeability of the blood–brain barrier and induces tight junction changes. *Front Neurosci*, 14:582324. https://doi.org/10.3389/fnins.2020.582324

Zhao Z, Nelson AR, Betsholtz C, et al., 2015. Establishment and dysfunction of the blood–brain barrier. *Cell*, 163(5):1064-1078. https://doi.org/10.1016/j.cell.2015.10.067

Zheng YY, Chen XJ, Wang Y, et al., 2024. Phenolic-enabled nanotechnology: a new strategy for central nervous system disease therapy. *J Zhejiang Univ-Sci B (Biomed & Biotechnol)*, 25(10):890-913. https://doi.org/10.1631/jzus.B2300839